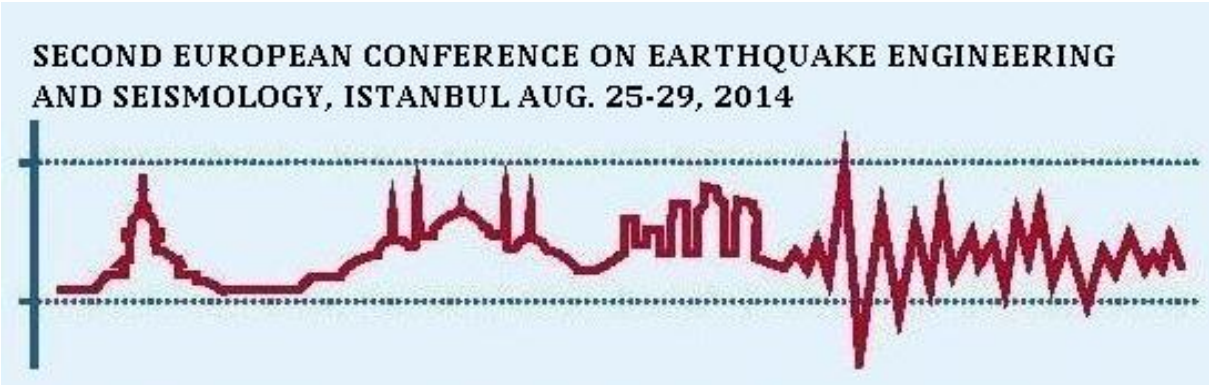

MODELING MACROSEISMIC INFORMATION FOR HISTORICAL EARTHQUAKES USING STOCHASTIC SIMULATION: THE CASE OF THE M=7.0, 1954 SOFADES (CENTRAL GREECE) EARTHQUAKE

Giannis PAPAZACHOS[1], Costas PAPAZACHOS[2], Efthimios LEKKAS[3], Andreas SKARLATOUDIS[4] and Harris KKALLAS[5]

ABSTRACT

This present study attempts to simulate the strong seismic motion of the M=7.0, 1954 Sofades earthquake (southern Thessaly basin, central Greece). Since no instrumental recordings were available for the specific earthquake, we have employed the macroseismic intensities (I_{MM} up to 9+) for this event, as they have been observed in the broader Thessaly area. For the simulation, a modified stochastic finite-fault method (EXSIM algorithm, Motazedian and Atkinson, 2005) was used, in order to reproduce the damage distribution of the 1954 Sofades earthquake.

The simulation approach attempts to combine existing earthquake information and appropriate scaling relations with surface geology, in order to investigate the efficiency and usefulness of the available macroseismic data (Papazachos et al., 1997). For the fault dimensions we utilized the calibrating equations for fault geometry from moment magnitude proposed for dip-slip faults by Papazachos et al. (2004) and Papazachos et al. (2006). In order to account for site-effects on the observed seismic motions, we have used a new digitized geological map for the broader Thessaly basin, using the 1:50000 geological maps of the Greek Institute of Geology and Mineral Exploration (IGME). The geological formations are grouped according to their age and mapped on appropriate soil classes, according to EC8.

Using the previous approach, we have estimated synthetic time series for different rupture scenarios. In order to compare the obtained stochastic motions with the historical (macroseismic) information, we have employed various relations between PGA and PGV (obtained from the stochastic records) with macroseismic intensity, allowing the generation of synthetic (stochastic) isoseismals. For each soil class, we test different site amplification factors, according to local geology (Skarlatoudis et al., 2003, Klimis et al., 1999). Moreover, a trial-and-error optimization of the fault position has been performed, using the available seismological information, as well as the published neotectonic data for this event and the broader southern Thessaly fault zone (Papastamatiou and Mouyaris, 1986, Mountrakis et al, 1993).

The results confirm the applicability of the proposed approach. The finally determined fault position is different than previously proposed, in agreement with the available neotectonic information. The observed macroseismic intensities are in very good agreement with the stochastic

[1] M.Sc. student, National and Kapodestrian University of Athens, Athens, jpapazahos@gmail.com
[2] Professor, Aristotle University of Thessaloniki, Thessaloniki, kpapaza@geo.auth.gr
[3] Professor, National and Kapodestrian University of Athens, Athens, elekkas@geol.uoa.gr
[4] Ph.D. Seismologist, Aristotle University of Thessaloniki, Thessaloniki, askarlat@geo.auth.gr
[5] M.Sc. Seismologist, Aristotle University of Thessaloniki, Thessaloniki, chkkalla@geo.auth.gr

simulation predictions, verifying both the usefulness of the approach, as well as of the macroseismic data used. Site-effects show an excellent correlation with the geological classification employed. Moreover, the constant amplification factors of Skarlatoudis et al. (2003) are in very good agreement with the observed amplifications, whereas the generic transfer functions proposed by Klimis et al. (1999) seem to lead to higher site amplifications, not observed in the real data, probably due to the very large thickness of Quaternary formations in the broader Thessaly basin.

INTRODUCTION

The broader Thessaly area is located at the back-arc area of the Aegean micro-plate and is one of the most seismically active areas of Greece. The area has been shown to expand in a more-or-less North-South direction (Fig. 1), with a velocity of ~1cm/year, due to the active stress field in the same direction. The result of this extension is the creation of normal faults mainly along its southern and northern borders, with dominant east-west strikes, which dip towards the north (along the southern Thessaly fault zone) or to the south (mostly in the northern Thessaly area, Caputo and Pavlides, 1993, Mountakis et al., 1993, Papazachos and Papazachou, 2002). This dominant E-W faulting pattern is also found along the western Thessaly border, were it co-exists with the N-S normal faults of the Hellenides mountain belt (e.g. Lekkas, 1988).

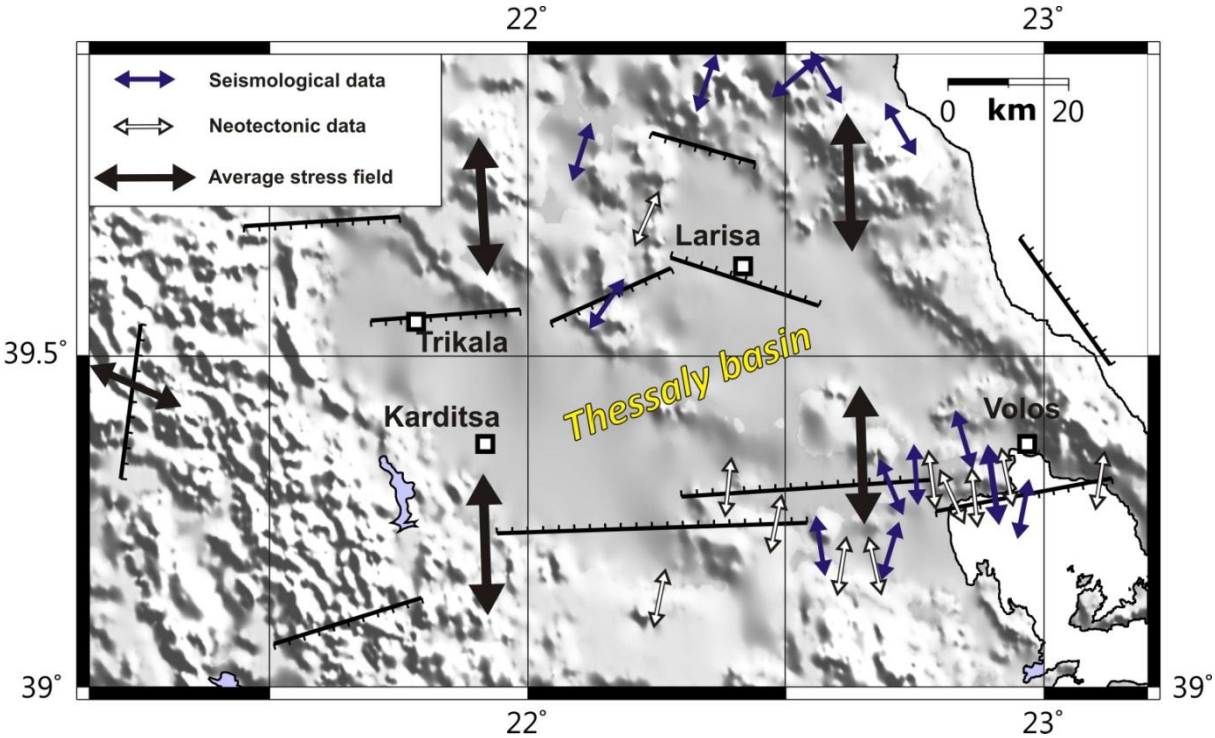

Figure 1. Extensional N-S trending stress field in the Thessaly basin, resulting in the generation of major active E-W striking faults (adopted from Papazachos et al., 2001). Small blue and white arrows denote T-axes from neotectonic and earthquake observations, respectively, while large black arrows depict the average stress field of the study area (modified from Panagiotopoulos and Papazachos, 2008).

The Thessaly basin, the largest basin in central Greece, has a well-known history of large earthquakes, with mainshocks having typical magnitudes between 6.0 and 7.0. The seismicity (instrumental and historic) follows the two discrete rupture zones of the Thessaly basin (e.g. Papazachos et al., 1993), also presented in Fig. 1. The northern zone, along Peneus river, is formed by small faults (typically < 25km) which are associated mainly with historical earthquakes with magnitudes up to ~6.5. For the southern Thessaly fault zone, along the southern boundaries of the Thessaly plain, the faults are relatively larger (up to ~50km), causing earthquakes with magnitudes up to M=7.0. During the 20th century, eight major seismic sequences with mainshock magnitudes equal or larger than 6.0 occurred in this area (1905, 1911, 1930, 1941, 1954, 1955, 1957, 1980), with the

M=7.0, 1954 Sofades earthquake being the most destructive event, resulting in heavy damages in the towns and villages of the broader southern Thessaly region (Papastamatiou and Mouyaris, 1986; Papazachos and Papazachou, 2002).

In the present work, we attempt to simulate the damage distribution for the 1954, M=7.0 event, using synthesized seismic motions, which are appropriately converted to macroseismic intensity, after incorporating the site-effect through the local geology. For this reason, we have applied the stochastic simulation method, which has been efficiently used for similar purposes during the last three decades.

The stochastic simulation method (originally developed as a point-source method) was initially proposed by Boore (1983) and then applied by a large number of researchers, in order to simulate the ground motion from seismic sources (e.g. Boore and Atkinson, 1987, Toro and MacGuire, 1987, Ou and Herrmann, 1990, Atkinson and Boore, 1995). EXSIM is a modified stochastic simulation algorithm, using finite-fault modelling with a dynamic corner frequency approach, as proposed by Motazedian and Atkinson (2005). In the present work, we have employed EXSIM to generate synthetic time series, also incorporating site-effects, leading to the estimation of Peak Ground Acceleration (PGA) and Peak Ground Velocity (PGV) from the synthetic time series, which were generated for specified earthquake fault rupture scenarios. The main advantage of the proposed approach is that it can reproduce realistic strong motion measures, although the modelled ruptures are specified by a few simple metrics, such as earthquake magnitude and distance, with options to include more detailed information on fault geometry and slip. In EXSIM, the fault is divided into equal sized subfaults, considered as point sources. The ground motions are calculated for each subfault using the original point-source method and then summed at the observation point. In most cases, also in the present work, a random rupture scenario has been considered in all simulations, though it is possible to introduce specific rupture scenarios (e.g. bi-directional, etc.)

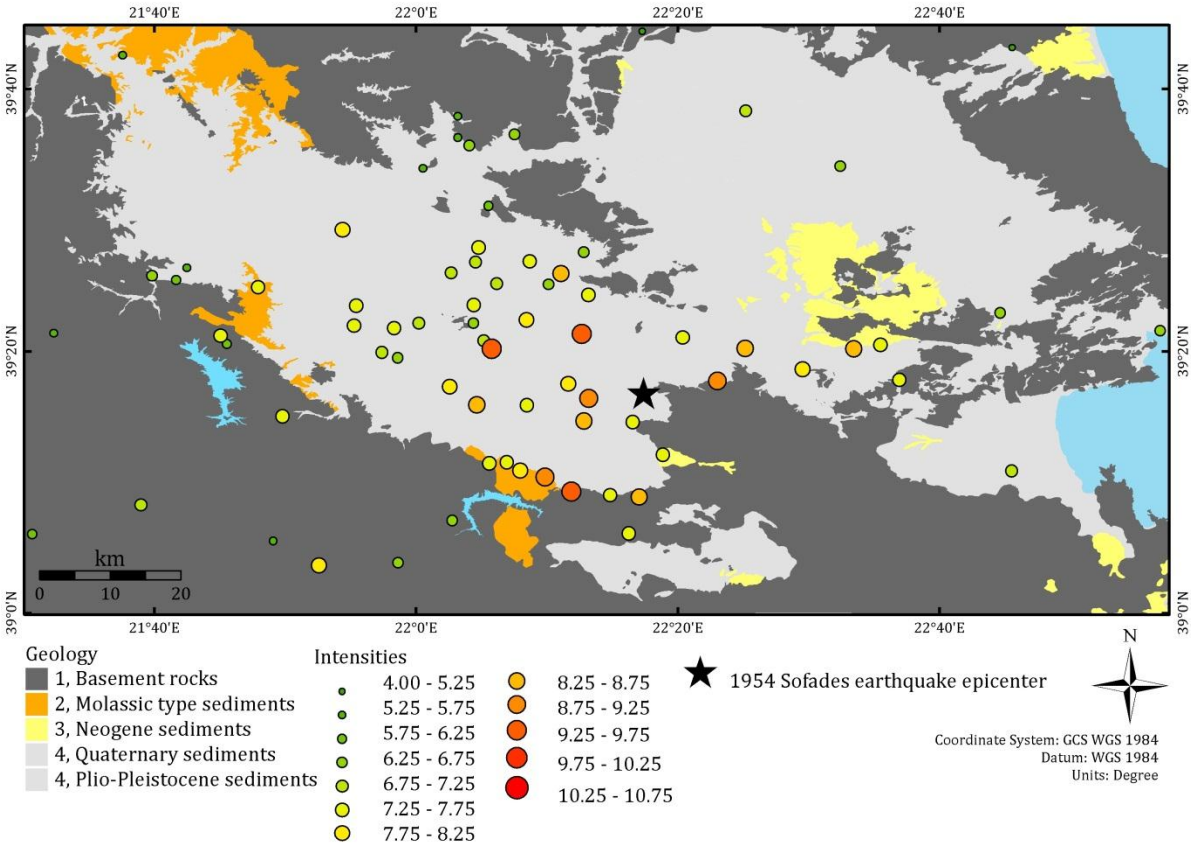

Figure 2. Observed macroseismic intensities (Modified Mercali scale) of the M=7.0, 1954 Sofades earthquake and main geological formation classes within the broader Thessaly basin area.

THE M=7.0 1954 SOFADES EARTHQUAKE

The M=7.0, 1954 Sofades earthquake occurred on April 30, 1954, and its epicenter was located at 39.28^o N, 22.29^o E (Fig.2). This event marked the beginning of a series of earthquakes along the southern Thessaly rupture zone, that also involved the destructive events of 1955 and 1957, which mostly affected the city of Volos and the whole eastern part of the southern Thessaly basin (Papastamatiou and Mouyaris, 1986).

Macroseismic data were collected from the published database of macroseismic information for the Aegean area (Papazachos et al., 1997), in order to reconstruct the observed intensities distribution among the settlements of the area. Observed intensities, ranging from 5 to 9+, were available for 75 settlements. The locations of these settlements were used as target sites for the simulations. The aftermath's descriptions by Papastamatiou and Mouyaris (1986) and Papazachos and Papazachou (2002) report damages in the prefectures of Karditsa, Larisa, Trikala, Phthiotida, Magnesia and Evritania. Overall, 6599 buildings were completely destroyed, 9154 were heavily damaged and 12920 were slightly damaged, while the town of Sofades, in the Karditsa prefecture, was almost entirely destroyed. In total, 25 people were killed and 157 were injured. Also, ground fissures, liquefaction phenomena and hydrological changes were observed in several places. The largest preceding shock occurred on April 25 (M=4.6) while the largest aftershock occurred on May 4 (M=5.7).

To assess the effect of the local site conditions on seismic motions, it is clear that detailed geophysical or geotechnical information cannot be employed, due to the scale of the study area. For this reason, we relied on the available geological information, which can provide an initial base for site-effect characterization. Geological formations were hand-digitized using the available Greek Institute of Geology and Mineral Exploration (IGME) maps (scale 1:50.000). The corresponding formations were clustered into four classes according to their age, hence their expected dynamic amplification behaviour, namely in: 1) Bedrock/Basement rocks (typically of Mesozoic-Paleogene age), 2) Molassic type sediments (Paleogene-Neogene age), 3) Neogene sediments and, 4) Quaternary-Plio/Pleistocene sediments (Fig.2). From the collected macroseismic information, nineteen (19) of the observation sites fall into class 1, four (4) of them into class 2 and fifty-two (52) into class 4. None of the observation sites were located on Neogene sediments (class 3).

STOCHASTIC SIMULATION

The fault position was initially constrained following the focal parameters (hypocenter and fault position, fault strike and dip, faulting type, etc.) provided by Papazachos et al. (2001). The fault's dimensions (length, L, and width, w) were estimated using Eq.1 and Eq.2, which have been proposed for the estimation of earthquake fault dimensions from moment magnitude for continental dip-slip faults (Papazachos et al. 2004, Papazachos et al. 2006). The dimensions (length, d_L and width, d_w) of each subfault were constrained from Eq.3, proposed by Beresnev and Atkinson (1999) and were slightly modified in order to scale with the calculated fault dimensions. The available field observations (Papastamatiou and Mouyaris, 1986, Mountrakis et al, 1993) showed a large number of surface fissures and small fault segments, without revealing a clear surface manifestation of the seismic fault along its length. For this reason, the depth of the upper edge of the fault was set to 1km, close to the surface. It should be noted that slightly larger depths of 2km and 3km were also tested but no significant differences were observed, though the larger depth (3km) resulted in systematic macroseismic intensity underestimation, suggesting that the adopted choice was appropriate.

$$LogL = 0.50M - 1.86 \quad (1)$$

$$Logw = 0.28M - 0.70 \quad (2)$$

$$Log\Delta l = -2 + 0.4M \quad (3)$$

For the simulation, the stress drop parameter was set to 70 bars (Boore and Joyner, 1997). The value 56 bars which has been proposed for normal and strike-slip faults in Greece by Margaris and Boore (1998) and is based in a relatively small number of data, was also tested, but returned very similar results, hence its effect could not be resolved, at least using the available macroseismic information. The crust's average shear wave velocity (beta) and density (rho) were derived from Papazachos et al. (1966). The rupture propagation velocity, V_{rup}, was set at a typical value of 0.8. Larger values (V_{rup}=0.9 and 0.95) were also tested but, again, returned similar results, with slightly lower synthetic macroseismic values for the southern Thessaly observation sites for the higher V_{rup} value. Different values were used for the high-frequency attenuation parameter kappa, k, according to the geology/soil class of each simulation site, as shown in Table 1. For the bedrock sites we used a smaller value than previously suggested for rock formations in Greece (Margaris and Boore, 1998) after a trial-and-error approach and taking into account our experience for k estimates from bedrock sites in the broader Aegean area. Table 2 summarizes all the parameters of the model adopted in the simulations.

Table 1. High-frequency attenuation parameter kappa, adopted for each geological soil class in the simulations

Geological group	kappa	Reference
1	0.015	Adopted after tests
2	0.044	Klimis et al. (1999)
4	0.066	Klimis et al. (1999)

Table 2. Parameters of the model adopted for all stochastic simulations for the strong motion of the M=7.0, 1954 Sofades earthquake

Strike	271°	d_L	6.286 km
Dip	47°	d_w	6 km
L	44 km	M_w	7
w	18 km	Stress	70 bars
Depth	1 km	beta	3.4 km/sec
Sub-faults	7x3	rho	2.7 gr/cm^3
V_{rup}	0.8	kappa	(as in Table 1)

Table 3. Spectral amplifications for EC8 soil category C according to Klimis et al. (1999), adopted for Molassic/Neogene sediments sites

Frequency (Hz)	Amplification factor	Frequency (Hz)	Amplification factor
0.11	1.076	2.67	2.898
0.15	1.107	3.51	3.029
0.31	1.253	5.40	3.243
0.50	1.504	8.01	3.446
0.66	1.763	12.24	3.659
1.78	2.633	24.16	3.990
1.10	2.219	34.04	4.121
2.11	2.751	62.50	4.306

The expected synthetic seismograms were initially simulated without considering the local site-effects (all formations were considered as basement rocks, class 1, without site amplifications). Following this step, the calculated PGA and PGV values were corrected for site-effects using the constant amplification factors proposed in the GMPE estimated by Skarlatoudis et al. (2003). For this

estimation it was assumed that bedrock, Molassic/Neogene, as well as Quaternary/Plio-Pleistocene sediments corresponded to UBC and EC8 soil categories A/B, C and D, respectively, as these are also considered by Skarlatoudis et al. (2003). Moreover, an additional simulation was performed, assuming the generic spectral amplifications factors shown in Tables 3 and 4, proposed for Greece for the site classes C and D by Klimis et al. (1999).

Table 4. Spectral amplifications for EC8 soil category D according to Klimis et al. (1999), adopted for Quaternary-Plio/Pleistocene sediments sites

Frequency (Hz)	Amplification factor	Frequency (Hz)	Amplification factor
0.09	1.125	1.52	3.909
0.10	1.142	1.98	4.113
0.19	1.307	3.09	4.376
0.35	1.742	5.34	4.722
0.46	1.993	7.07	4.918
0.50	2.094	9.39	5.051
1.03	3.347	14.87	5.195
1.15	3.536	40.50	5.461

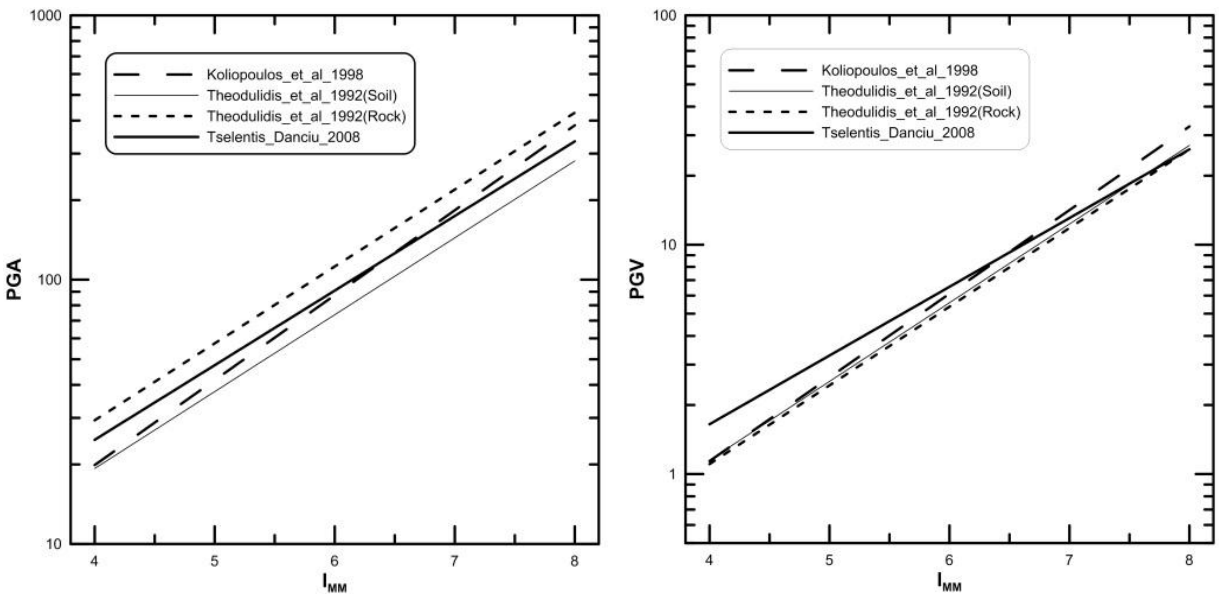

Figure 3. Comparison of published scaling relations (Theodulidis et al., 1992; Koliopoulos et al., 1998; Tselentis and Danciu, 2008) between I_{MM} and PGA (left) and PGV (right) proposed for the Greek area.

The final step for the simulation modeling corresponded to the estimation of the expected macroseismic intensities from the synthetic stochastic seismograms. Though this approach is not straightforward, we have adopted a standard approach, where the PGA and PGV values from the synthetic waveforms were converted them macroseismic intensities (Modified Mercali scale, I_{MM}). For this reason we employed the proposed relations for the Greek area between PGA/PGV and I_{MM} by Theodulidis and Papazachos (1992), Koliopoulos et al., (1998) and Tselentis and Danciu (2008). A comparison of the corresponding scaling relations is presented in Fig.3. From both plots it is evident that the relations proposed by Tselentis and Danciu (2008) are close to the average of all examined relations, especially for PGA. For this reason, as well as since it was the most recently developed approach, we adopted for the final I_{MM} assessment the average I_{MM} values defined using the corresponding conversion relations (Eq.4 and Eq.5) proposed by Tselentis and Danciu (2008).

$$I_{MM} = -0.946 + 3.563 \log PGA \tag{4}$$

$$I_{MM} = 3.3 + 3.358 \log PGV \tag{5}$$

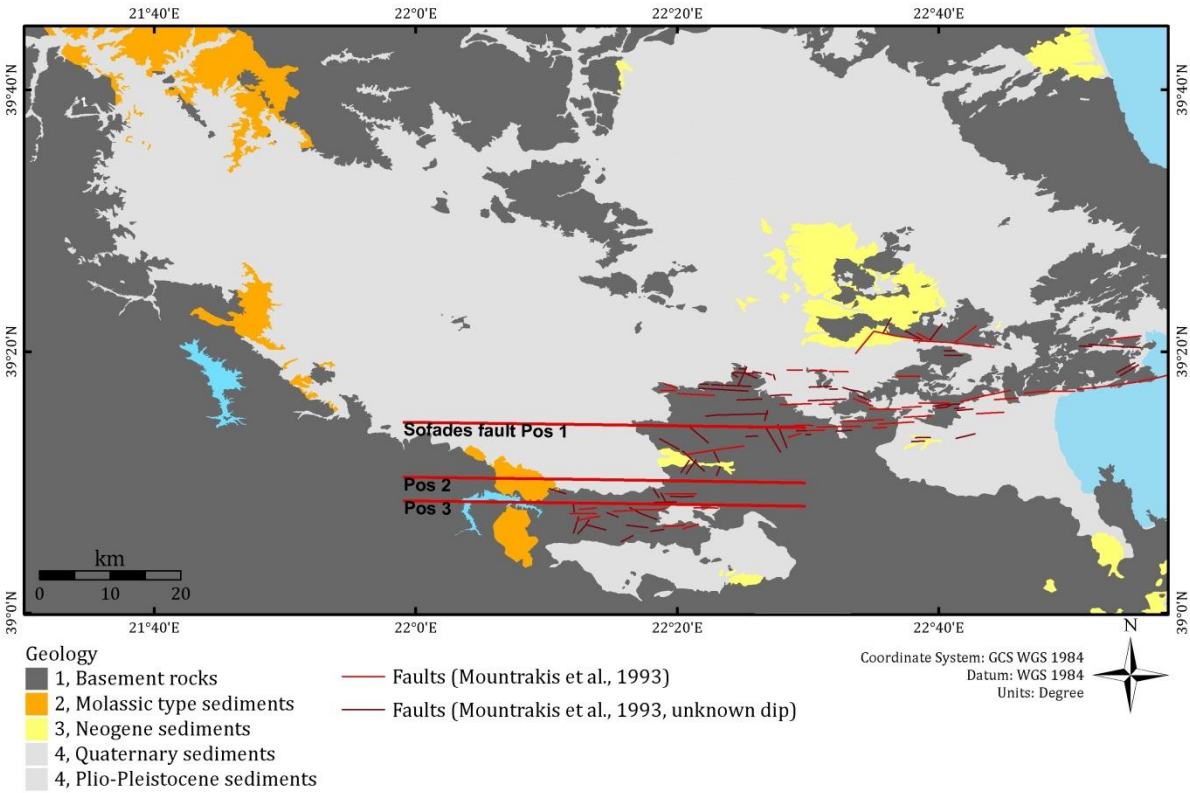

Figure 4. The three candidate positions for the upper Sofades fault edge considered in the present study for the 1954 event. The main active faults in southern Thessaly, proposed by Mountrakis et al. (1993), are also depicted.

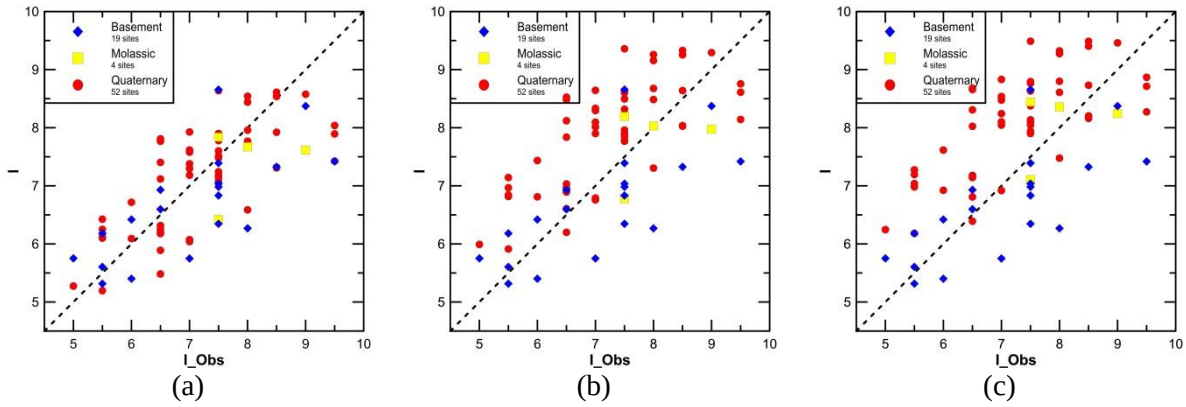

Figure 5. Comparison of modeled, I, against observed, I_Obs, macroseismic intensities for fault position 1 scenario (see Fig. 4). (a) No site-effects. (b) Using the constant amplification factors of Skarlatoudis et al. (2003). (c) Using the generic spectral amplifications proposed by Klimis et al. (1999).

For the initial simulation we adopted the fault position proposed by Papazachos et al. (2001), depicted as Pos.1 in Fig.4. The results from this initial simulation, presented in Fig.5, showed significant deviations between observed and synthetic intensities. These differences are observed both without site amplifications, as well as when using the constant site amplification factors proposed by Skarlatoudis et al. (2003), and the generic spectral amplifications suggested by Klimis et al. (1999). In general, the results show that the modeled intensities for bedrock sites (blue diamonds in Fig.5) are

lower than the observed intensities. The opposite is observed for soil sites, with synthetic macroseismic intensities (no site-effect amplification, Fig.5a) showing much larger values than the observed values, contrary to what would be expected for these sites, which are expected to exhibit significant site amplifications. Due to this discrepancy, the bias between synthetic and observed macroseismic intensities becomes worse when using site-effect amplifications (Fig.5b and Fig.5c).

In order to explain this discrepancy, it is clear that any simulation scenario would require a reduction of the synthetic macroseismic intensities for the soft soil (essentially Quaternary/Plio-Pleistocene) sites, and an opposite increase for bedrock sites. This pattern can be partly fulfilled if the fault's upper edge would be located southern than the initial position examined, being in better agreement with the mapped active faults of the southern Thessaly fault zone (Mountrakis et al., 1993), as these are presented in Fig. 4. For this reason two additional possible fault positions were considered, depicted as Pos.2 and Pos.3 in Fig.4. As Fig.6 indicates, simulations using the second fault position (Pos.2) also resulted in significant deviations between observed and synthetic macroseismic intensities.

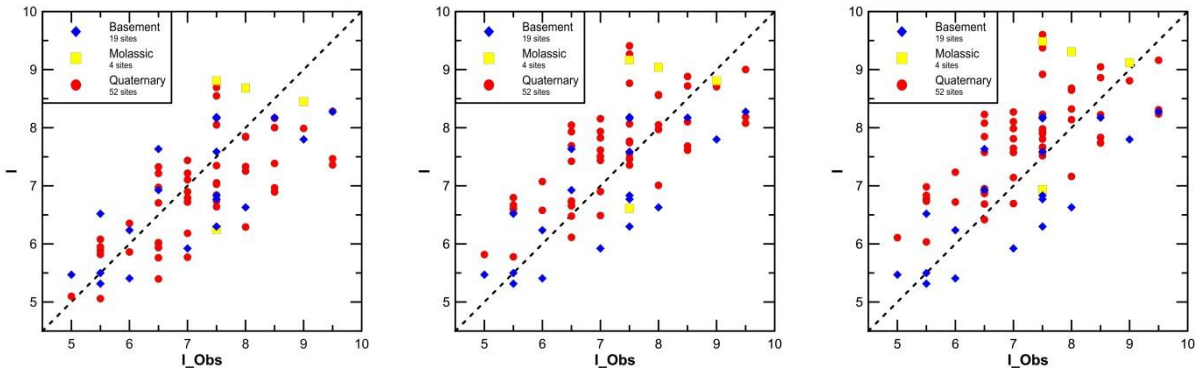

(a) (b) (c)

Figure 6. Same as Fig. 5, for the second fault position simulation (Pos.2 in Fig. 4).

The third fault position examined (Pos.3 in Fig.4), which was constrained by the observed surface ruptures and neotectonic faulting of the southern Thessaly basin (Papastamatiou and Mouyaris, 1986, Caputo and Pavlides, 1993, Mountrakis et al, 1993, also shown in Fig.4) led to the best results, as is presented in Fig.7. As can be seen from Fig.7a, the synthetic and macroseismic intensities correlate well when no site amplifications are considered. The observed agreement for bedrock sites suggests that the fault position is optimally placed, in agreement with the available neotectonic information. However, the soil sites (mostly Quaternary/Plio-Pleistocene sites, class D) show significantly higher observed intensities, when no site amplifications are considered for the stochastic simulation results. This observation confirms the presence of significant site amplification effects for class D formations, as expected.

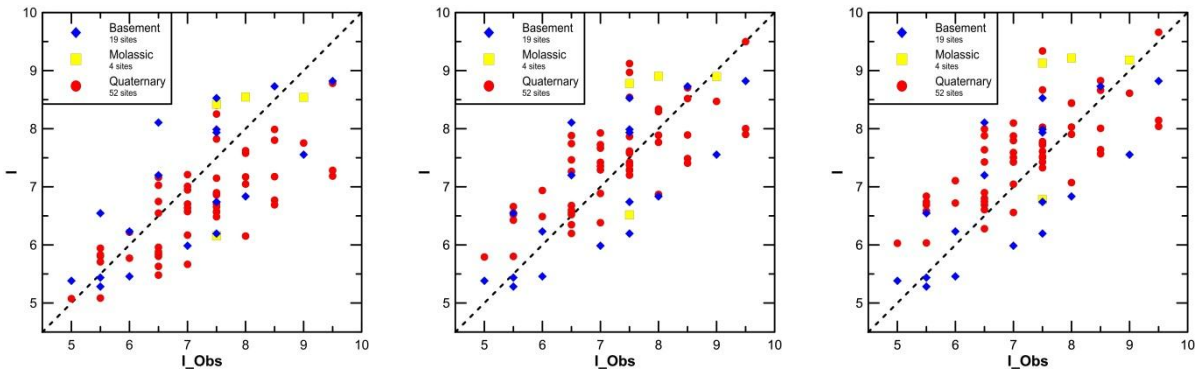

(a) (b) (c)

Figure 7. Same as Fig. 5, for the third fault position simulation (Pos.3 in Fig. 4).

It should be noticed that performing simulations using the amplification factors proposed by Klimis et al. (1999), in an attempt to account for this pattern, has led to a systematic overestimation of

macroseismic intensities for these mainly Quaternary formation sites (Fig.7c), especially for the central Thessaly basin part. Selected HVSR measurements performed in the southern Thessaly basin showed that the recovered resonance frequencies for the central section of the basin (Karditsa area) exhibit a very low resonant frequency (~0.4Hz, as shown in Fig.8), probably due to the significant thickness of the Quaternary deposits. This low frequency amplification is very different that the corresponding typical (generic) amplification factors proposed by Klimis et al. (1999) for EC8 class D formations (see Table 4), which can be considered as the main reason for the observed discrepancy and macroseismic intensity overestimation. The optimal results have been obtained for fault position 3 (Pos.3 in Fig. 4), using the constant amplification factors for PGA and PGV proposed by Skarlatoudis et al. (2003) for the broader Aegean area. Macroseismic intensities for both bedrock and Quaternary formation sites show a very good correlation between predicted and observed intensities (Fig. 7b).

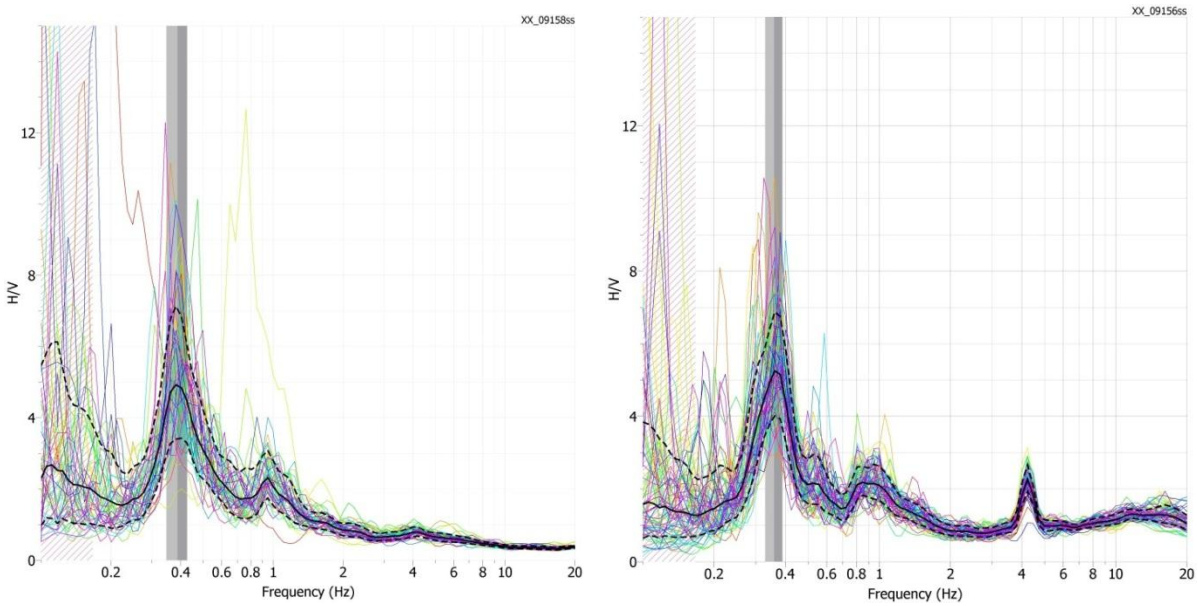

Figure 8. HVSR variation with frequency (data processing with the Geopsy software, http://www.geopsy.org/), showing a low resonant frequency (~0.35-0.4Hz) for two different positions within the Karditsa area (Quaternary formation sites).

In order to assess the effect of the performed modeling for the broader Thessaly area, we have adopted the final modeling parameters (Table 1, Pos.3, constant amplification factors for soil formations, etc.) and performed computations for a grid of target points with 4km spacing, in order to estimate the expected damage distribution of the 1954 event, in terms of macroseismic intensities, throughout the whole study area. The final damage distribution map for bedrock (no site amplification) and using appropriate site amplification are presented in Fig. 9. The results confirm the effect of the fault geometry, as well as local geology on the expected (and observed) seismic motions, with significant modifications of the observed damage pattern due to the presence of local site-effects. More specifically, the hanging wall fault area is exhibiting higher seismic motion levels, which are further enhanced for the largest part of the southwestern Quaternary Thessaly basin.

CONCLUSIONS

This present study shows that it is possible to efficiently simulate the rupture of historical earthquakes by using macroseismic data and contemporary simulation tools, such as stochastic simulation algorithms (e.g. EXSIM) and by applying appropriate relations converting PGA and PGV values (from synthetic waveforms) to macroseismic intensities, I_{MM} (e.g. Tselentis and Danciu, 2008). The simulations also have verified that the use of equations for fault dimensions calibration (e.g. Papazachos et al. 2004, Papazachos et al. 2006) leads to realistic results, even for historical earthquakes.

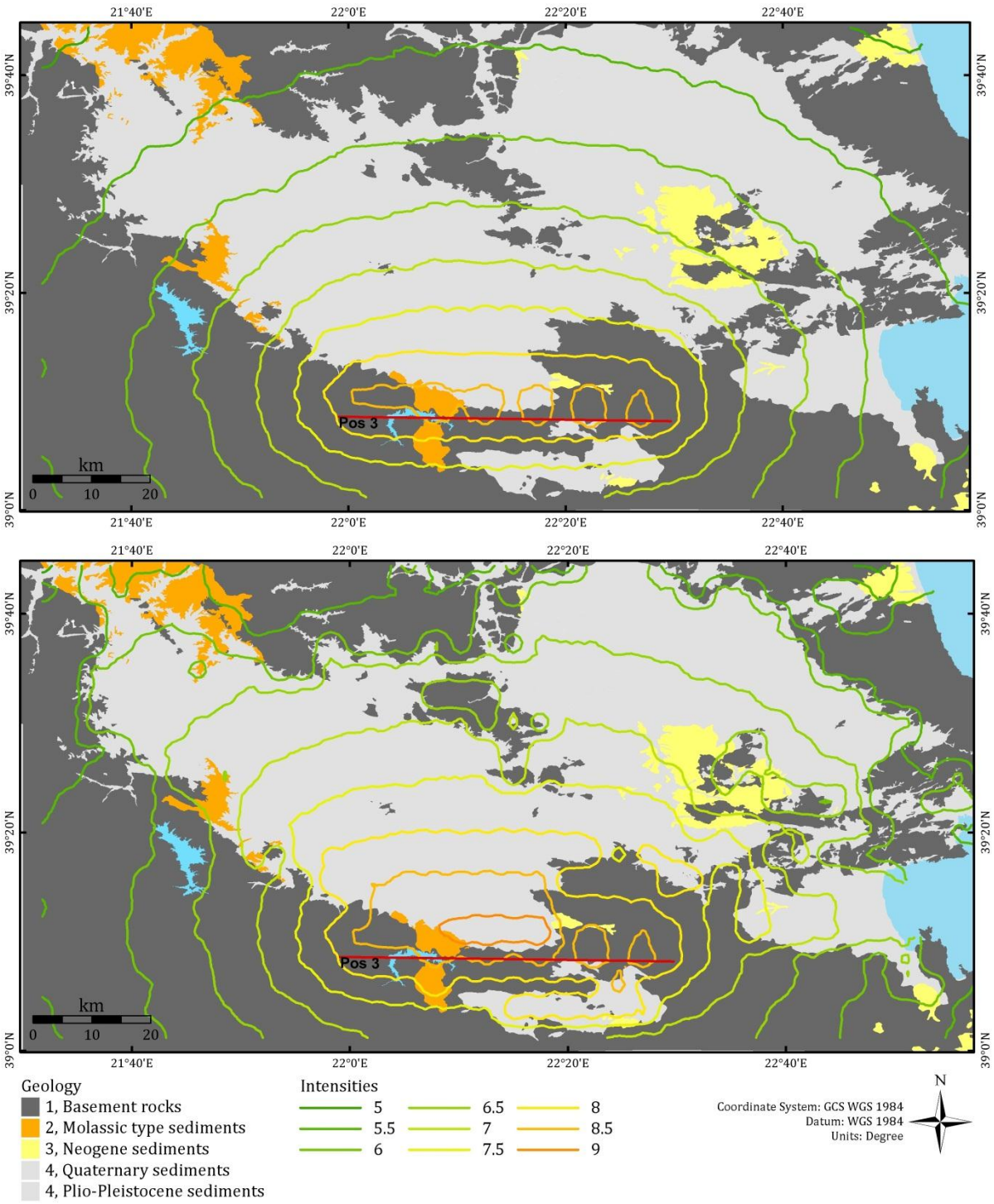

Figure 9. Estimated macroseismic intensities contours (synthetic isoseismals) for the M=7.0, 1954 Sofades event, considering the optimal fault position 3 (see Fig.4), without the use of site amplifications (upper figure) and with the use of the constant PGA/PGV amplification factors of Skarlatoudis et al. (2003) (lower figure).

From the performed simulations, it can be suggested that the originally proposed position for the Sofades fault position, as constrained by the already published information, is probably incorrect. Using the simulated macroseismic intensities, especially for bedrock formations which are not affected by site-effects, it was possible to relocate the fault towards the southern edge of the southwest Thessaly basin. The proposed fault position (Pos.3 in Fig. 4) is in very good agreement with the available neotectonic data for the area (e.g. Mountrakis et al., 1993). Moreover, the obtained results confirmed the significant effect of local geology on strong seismic motion, showing important

differentiation in the ground response of basements rocks against Quaternary/Plio-Pleistocene sediment sites.

The results obtained in this study have showed that the generic transfer functions proposed by Klimis et al. (1999) for the area of Greece, could not realistically describe the observed site-effects, resulting in very high amplifications for the Quaternary/Plio-Pleistocene sediments. This discrepancy is most probably due to the high Quaternary sedimentary thickness of the Thessaly basin, which leads to low-frequency amplifications that are not adequately reflected in the generic transfer functions, in agreement with the available H/V information. On the contrary, the constant amplification factors proposed by Skarlatoudis et al. (2003) for PGA and PGV resulted in satisfactory simulation results and realistic site amplification estimates.

REFERENCES

Atkinson, G.M. and Boore, D.M. (1995). "Ground-motion relations for eastern North America", *Bull. Seism. Soc. Am.*, 85:17-30

Beresnev I.A. and Atkinson G.M. (1999). "Generic finite-fault model for ground-motion prediction in eastern North America**",** *Bull. Seism. Soc. Am.*, 89:608-625

Boore, D.M. (1983) "Stochastic simulation of high-frequency ground motions based on seismological models of the radiated spectra", *Bull. Seism. Soc. Am*., 73:1865–1894.

Boore, D.M. and Atkinson, G.M. (1987) "Stochastic prediction of ground motion and spectral response parameters at hard-rock sites in eastern north America", *Bull. Seism. Soc. Am*., 77:440-467.

Boore, D.M. and Joyner, W.B. (1997). "Site amplifications for generic rock sites", *Bull. Seism. Soc. Am., 87:327-341*

Caputo, R., and Pavlides, S. (1993). "Late Cainozoic geodynamic evolution of Thessaly and surroundings (central-northern Greece)." *Tectonophysics*, 223(3): 339-362.

Klimis, N.S., Margaris, B.N., and Koliopoulos, P.K. (1999) "Site-dependent amplification functions and response spectra in Greece", Journal of Earthquake Engineering, 3(02):237-270.

Koliopoulos, P.K., Margaris, B.N., and Klimis, N.S. (1998). "Duration and energy characteristics of Greek strong motion records". *Journal of Earthquake Engineering*, 2(3): 391-417.

Lekkas, E. (1988). "Geological structure and geodynamic evolution of the Koziakas mountain range (western Thessaly)." *Ph.D. Thesis, University of Athens*, Department of Geology: 281pp.

Margaris, B.N. and Boore D.M. (1998). "Determination of $\Delta\sigma$ and κ_0 from response spectra of large earthquakes in Greece", *Bull. Seism. Soc. Am.,88:170-182*

Motazedian, D. and Atkinson, G.M. (2005) "Stochastic Finite-Fault Modeling Based on a Dynamic Corner Frequency", *Bull. Seism. Soc. Am*., 95:995–1010.

Mountrakis, D., Kilias, A., Pavlides, S., Zouros, N., Spyropoulos, N., Tranos, M. and Soulakelis, N. (1993) "Field study of the southern Thessaly highly active fault zone", *Proceedings of the 2nd Congress of the Hellenic Geophysical Union, May 5–8, 1993, Florina, Greece*, 2:603–614.

Ou G. and Herrmann R.B. (1990). "A statistical model for ground motion produced by earthquakes at local and regional distances", *Bull. Seism. Soc. Am., 80:1397-1417*

Panagiotopoulos, D.G. and C.B. Papazachos (2008), "Application of modern methods for assessing the seismicity of Karditsa", *Proc. of the 1st development conf. of Karditsa*, 8-10 Feb 2008, Karditsa, Greece.

Papastamatiou D. and Mouyaris, N. (1986) "The earthquake of April 30, 1954, in Sophades (Central Greece)", *Geophys. J. R. astr. Soc*., 87:885–895.

Papazachos, B.C., and Papazachou, C. (2002). "The Earthquakes of Greece", *Ziti Publ.*, Thessaloniki, Greece, 317 pp

Papazachos, B.C., Comninakis, P.E., & Drakopoulos, J.C. (1966). Preliminary results of an investigation of crustal structure in southeastern Europe. *Bull. Seism. Soc. Am*., 56(6), 1241-1268.

Papazachos B.C., Hatzidimitriou, P.M., Karakaisis, G.F., Papazachos,C.B. and Tsokas, G.N. (1993) "Rupture zones and active crustal deformation in southern Thessalia, central Greece.", *Boll. Geof. Teor. Appl.*, 35:363 - 374.

Papazachos, B.C., Papaioannou, Ch., Papazachos, C.B. and Savvaidis, A.S. (1997) "Atlas of isoseismal maps for strong shallow earthquakes in Greece and surrounding area (426BC-1995)", *Ziti Publ., Thessaloniki*, 192pp.

Papazachos, B.C., Mountrakis, D.M., Papazachos, C.B., Tranos, M.D., Karakaisis, G.F., and Savvaidis, A.S. (2001) "The faults which have caused the known major earthquakes in Greece and surrounding region between the 5th century BC and today". In: *Proceedings of 2nd National Conference Anti-Seismic Engineering and Technical Seismology (pp. 17-26), Athens, Greece: Technical Chamber of Greece*.

Papazachos, B.C., Scordilis, E.M., Panagiotopoulos, D.G., Papazachos, C.B. and Karakaisis, G.F. (2004) "Global relations between seismic fault parameters and earthquake moment", *Bull. Geol. Soc. Greece*, 36:1482-1489.

Papazachos, B.C., Karakaisis, G.F., Papazachos, C.B., and Scordilis, E.M. (2006) "Perspectives for earthquake prediction in the Mediterranean and contribution of geological observations", In: *Tectonic Development of the Eastern Mediterranean Region. (From: Robertson, A.H.F. & Mountrakis, D., eds), Publ. Geol. Soc., London*, 260:689–707.

Skarlatoudis, A.A., Papazachos, C.B., Margaris, B.N., Theodulidis, N., Papaioannou, Ch., Kalogeras, I., Scordilis E.M. and Karakostas, V. (2003) "Empirical peak ground motion predictive relations for shallow earthquakes in Greece", *Bull. Seism. Soc. Am*., 93:2591-2603.

Theodulidis, N.P., and B.C. Papazachos. "Dependence of strong ground motion on magnitude-distance, site geology and macroseismic intensity for shallow earthquakes in Greece: I, Peak horizontal acceleration, velocity and displacement", *Soil Dynamics and Earthquake Engineering*, 11(7): 387-402.

Toro, G.R., and R.K. McGuire. "An investigation into earthquake ground motion characteristics in eastern North America", *Bull. Seism. Soc. Am*., 77(2): 468-489.

Tselentis, G.A. and Danciu, L. (2008) "Empirical relationships between modified Mercalli intensity and engineering ground-motion parameters in Greece.", *Bull. Seism. Soc. Am*., 98(4):1863-1875.